Angular analysis of $\mathrm{B} \to \mathrm{K}^{(*)}\mu\mu$ decays at CMS

Alessio Boletti
on behalf of CMS collaboration

Università degli Studi di Padova & INFN Padova

BEAUTY2019
Ljubljana, 2 October 2019

Introduction

- Flavour-changing neutral current decays $b \to s\ell^+\ell^-$ are doubly suppressed in the Standard Model
- Good laboratory to probe new-physics effects, through angular analysis and branching fraction measurement

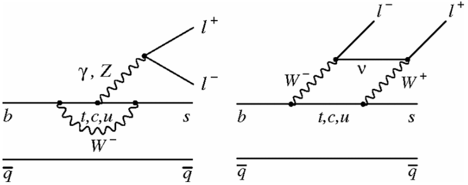

- The $\mathrm{B}^0 \to \mathrm{K}^{*0}\mu\mu$ decay
  - Flavour eigenstate (B^0/ $\overline{\mathrm{B}}^0$) can be identified through the $\mathrm{K}^{*0} \to \mathrm{K}^-\pi^+$ decay
  - allows measuring a large set of angular parameters, sensitive to Wilson coefficients $\mathcal{C}_7^{(\prime)}$, $\mathcal{C}_9^{(\prime)}$, $\mathcal{C}_{10}^{(\prime)}$, $\mathcal{C}_{S,P}^{(\prime)}$
- The $\mathrm{B}^+ \to \mathrm{K}^+\mu\mu$ decay
  - allows measuring the muon forward-backward asymmetry
- Both channels are experimentally accessible, thanks to the fully-charged final states and easy-to-identify muon pair

Angular analyses in CMS

1. $B^0 \rightarrow K^{*0}\mu\mu$ analysis with Run 1 data

2. $B^+ \rightarrow K^+\mu\mu$ analysis with Run 1 data

3. Prospects for the $B^0 \rightarrow K^{*0}\mu\mu$ analysis at HL-LHC

$B^0 \to K^{*0}(892)\mu^+\mu^- \to K^+\pi^-\mu^+\mu^-$ angular analysis

Phys. Lett. B 781 (2018) 517-541
arXiv:1710.02846

- Fully described by three angles: $\theta_\ell, \theta_K, \phi$ and $q^2 = M^2_{\mu\mu}$
- Robust SM calculations of several angular parameters in most of the phase space
  - forward-backward asymmetry of the muons, $\boldsymbol{A_{FB}}$
  - longitudinal polarisation fraction of the K^{*0}, $\boldsymbol{F_L}$
  - set of clean parameters, $\boldsymbol{P_i^{(\prime)}}$
- The q^2 range has been divided in 9 bins
  - 7 signal bins, in each of them the angular analysis is performed independently
  - 2 control-region bins, covering the two resonant decays
    - $B^0 \to J/\psi K^{*0}$
    - $B^0 \to \psi(2S)K^{*0}$

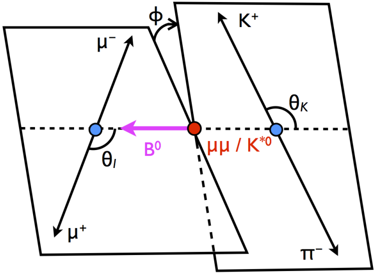

Previous CMS analyses

2011 data: Phys. Lett. B 727 (2013) 77
2012 data: Phys. Lett. B 753 (2016) 424

- Two analyses were performed and published by CMS with 2011 and 2012 data
- The parameter space was reduced by integrating over the ϕ angular variable
- A_{FB} and F_L parameters and differential branching fraction were measured
- No deviations from SM prediction
- The analysis presented here is performed on the same dataset and uses the same selection criteria as the previous 2012 analysis

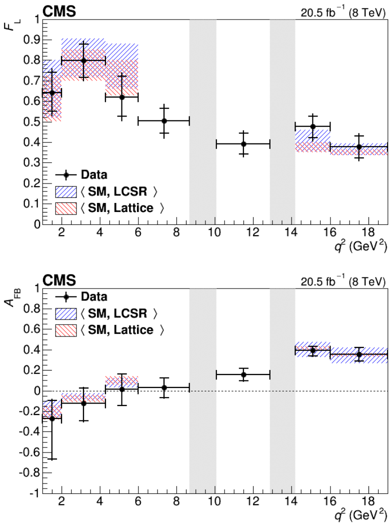

Angular decay rate

- Final state $K^+\pi^-\mu^+\mu^-$ has contribution from P-wave (K^{*0}), S-wave, and interference
- In total, the decay rate has 14 parameters: fold around $\phi = 0$ and $\theta_\ell = \pi/2$ to reduce them

$$\frac{1}{\mathrm{d}\Gamma/\mathrm{d}q^2}\frac{\mathrm{d}^4\Gamma}{\mathrm{d}q^2\mathrm{d}\cos\theta_l\mathrm{d}\cos\theta_\mathrm{K}\mathrm{d}\phi} = \frac{9}{8\pi}\left\{\frac{2}{3}\left[(F_\mathrm{S} + A_\mathrm{S}\cos\theta_\mathrm{K})\left(1-\cos^2\theta_l\right) + A_\mathrm{S}^5\sqrt{1-\cos^2\theta_\mathrm{K}}\sqrt{1-\cos^2\theta_l}\cos\phi\right]\right.$$
$$+ (1-F_\mathrm{S})\left[2F_\mathrm{L}\cos^2\theta_\mathrm{K}\left(1-\cos^2\theta_l\right) + \frac{1}{2}(1-F_\mathrm{L})\left(1-\cos^2\theta_\mathrm{K}\right)\left(1+\cos^2\theta_l\right)\right.$$
$$+ \frac{1}{2}P_1(1-F_\mathrm{L})(1-\cos^2\theta_\mathrm{K})(1-\cos^2\theta_l)\cos 2\phi$$
$$\left.\left. + 2P_5'\cos\theta_\mathrm{K}\sqrt{F_\mathrm{L}(1-F_\mathrm{L})}\sqrt{1-\cos^2\theta_\mathrm{K}}\sqrt{1-\cos^2\theta_l}\cos\phi\right]\right\}$$

- 6 angular parameters left:
  fit with all of them free to float not possible (low statistics, proximity of physical boundaries)

Angular decay rate

- Final state $K^+\pi^-\mu^+\mu^-$ has contribution from P-wave (K^{*0}), S-wave, and interference
- In total, the decay rate has 14 parameters: fold around $\phi = 0$ and $\theta_\ell = \pi/2$ to reduce them

$$\frac{1}{d\Gamma/dq^2}\frac{d^4\Gamma}{dq^2 d\cos\theta_l d\cos\theta_K d\phi} = \frac{9}{8\pi}\left\{\frac{2}{3}\left[(F_S + A_S\cos\theta_K)\left(1-\cos^2\theta_l\right) + A_S^5\sqrt{1-\cos^2\theta_K}\sqrt{1-\cos^2\theta_l}\cos\phi\right]\right.$$
$$+(1-F_S)\left[2F_L\cos^2\theta_K\left(1-\cos^2\theta_l\right) + \frac{1}{2}(1-F_L)\left(1-\cos^2\theta_K\right)\left(1+\cos^2\theta_l\right)\right.$$
$$+\frac{1}{2}P_1(1-F_L)(1-\cos^2\theta_K)(1-\cos^2\theta_l)\cos 2\phi$$
$$\left.\left.+2P_5'\cos\theta_K\sqrt{F_L(1-F_L)}\sqrt{1-\cos^2\theta_K}\sqrt{1-\cos^2\theta_l}\cos\phi\right]\right\}$$

- 6 angular parameters left:
  fit with all of them free to float not possible (low statistics, proximity of physical boundaries)

Angular decay rate

- Final state $K^+\pi^-\mu^+\mu^-$ has contribution from P-wave (K^{*0}), S-wave, and interference
- In total, the decay rate has 14 parameters: fold around $\phi = 0$ and $\theta_\ell = \pi/2$ to reduce them

$$\frac{1}{\mathrm{d}\Gamma/\mathrm{d}q^2}\frac{\mathrm{d}^4\Gamma}{\mathrm{d}q^2\mathrm{d}\cos\theta_l\mathrm{d}\cos\theta_K\mathrm{d}\phi} = \frac{9}{8\pi}\left\{\frac{2}{3}\left[(F_S + A_S\cos\theta_K)\left(1-\cos^2\theta_l\right) + A_S^5\sqrt{1-\cos^2\theta_K}\sqrt{1-\cos^2\theta_l}\cos\phi\right]\right.$$
$$+ (1-F_S)\left[2F_L\cos^2\theta_K\left(1-\cos^2\theta_l\right) + \frac{1}{2}(1-F_L)\left(1-\cos^2\theta_K\right)\left(1+\cos^2\theta_l\right)\right.$$
$$+ \frac{1}{2}P_1(1-F_L)(1-\cos^2\theta_K)(1-\cos^2\theta_l)\cos 2\phi$$
$$\left.\left. + 2P_5'\cos\theta_K\sqrt{F_L(1-F_L)}\sqrt{1-\cos^2\theta_K}\sqrt{1-\cos^2\theta_l}\cos\phi\right]\right\}$$

- 6 angular parameters left:
  fit with all of them free to float not possible (low statistics, proximity of physical boundaries)
- F_L, F_S, and A_s fixed from previous CMS measurement

Angular decay rate

- Final state $K^+\pi^-\mu^+\mu^-$ has contribution from P-wave (K^{*0}), S-wave, and interference
- In total, the decay rate has 14 parameters: fold around $\phi = 0$ and $\theta_\ell = \pi/2$ to reduce them

$$\frac{1}{\mathrm{d}\Gamma/\mathrm{d}q^2}\frac{\mathrm{d}^4\Gamma}{\mathrm{d}q^2\mathrm{d}\cos\theta_l\mathrm{d}\cos\theta_K\mathrm{d}\phi} = \frac{9}{8\pi}\left\{\frac{2}{3}\left[(F_S + A_S\cos\theta_K)\left(1-\cos^2\theta_l\right) + A_S^5\sqrt{1-\cos^2\theta_K}\sqrt{1-\cos^2\theta_l}\cos\phi\right]\right.$$
$$+ (1-F_S)\left[2F_L\cos^2\theta_K\left(1-\cos^2\theta_l\right) + \frac{1}{2}(1-F_L)\left(1-\cos^2\theta_K\right)\left(1+\cos^2\theta_l\right)\right.$$
$$+ \frac{1}{2}P_1(1-F_L)(1-\cos^2\theta_K)(1-\cos^2\theta_l)\cos 2\phi$$
$$\left.\left. + 2P_5'\cos\theta_K\sqrt{F_L(1-F_L)}\sqrt{1-\cos^2\theta_K}\sqrt{1-\cos^2\theta_l}\cos\phi\right]\right\}$$

- 6 angular parameters left:
  fit with all of them free to float not possible (low statistics, proximity of physical boundaries)
- F_L, F_S, and A_s fixed from previous CMS measurement
- P_1 and P_5' measured, A_s^5 nuisance parameter

Fit pdf description

$$\begin{aligned}\mathrm{p.d.f.}(m, \cos\theta_{\mathrm{K}}, \cos\theta_l, \phi) = Y_S^C \cdot \Big(& S^R(m) \cdot S^a(\cos\theta_{\mathrm{K}}, \cos\theta_l, \phi) \cdot \epsilon^R(\cos\theta_{\mathrm{K}}, \cos\theta_l, \phi) \\ & + \frac{f^M}{1 - f^M} \cdot S^M(m) \cdot S^a(-\cos\theta_{\mathrm{K}}, -\cos\theta_l, -\phi) \cdot \epsilon^M(\cos\theta_l, \cos\theta_{\mathrm{K}}, \phi)\Big) \\ & + Y_B \cdot B^m(m) \cdot B^{\cos\theta_{\mathrm{K}}}(\cos\theta_{\mathrm{K}}) \cdot B^{\cos\theta_l}(\cos\theta_l) \cdot B^{\phi}(\phi).\end{aligned}$$

Fit pdf description

$$\begin{aligned}\mathrm{p.d.f.}(m, \cos\theta_K, \cos\theta_l, \phi) = Y_S^C \cdot \Big(& S^R(m) \cdot S^a(\cos\theta_K, \cos\theta_l, \phi) \cdot \epsilon^R(\cos\theta_K, \cos\theta_l, \phi) \\ & + \frac{f^M}{1-f^M} \cdot S^M(m) \cdot S^a(-\cos\theta_K, -\cos\theta_l, -\phi) \cdot \epsilon^M(\cos\theta_l, \cos\theta_K, \phi) \Big) \\ & + Y_B \cdot B^m(m) \cdot B^{\cos\theta_K}(\cos\theta_K) \cdot B^{\cos\theta_l}(\cos\theta_l) \cdot B^{\phi}(\phi).\end{aligned}$$

Signal components for correctly-tagged
and mis-tagged events, each composed by:

- double-Gaussian mass shape
- angular decay rate
- 3D efficiency function
  (using non-parametric Kernel-Density-Estimator)

Flavour state assignment based on $M(K\pi)$ value

- mis-tagged event fraction 14%, measured on MC

Fit pdf description

$$\mathrm{p.d.f.}(m, \cos\theta_K, \cos\theta_l, \phi) = Y_S^C \cdot \Big(S^R(m) \cdot S^a(\cos\theta_K, \cos\theta_l, \phi) \cdot \epsilon^R(\cos\theta_K, \cos\theta_l, \phi) + \frac{f^M}{1-f^M} \cdot S^M(m) \cdot S^a(-\cos\theta_K, -\cos\theta_l, -\phi) \cdot \epsilon^M(\cos\theta_l, \cos\theta_K, \phi)\Big) + Y_B \cdot \boxed{B^m(m) \cdot B^{\cos\theta_K}(\cos\theta_K) \cdot B^{\cos\theta_l}(\cos\theta_l) \cdot B^{\phi}(\phi).}$$

Signal components for correctly-tagged and mis-tagged events, each composed by:

- double-Gaussian mass shape
- angular decay rate
- 3D efficiency function (using non-parametric Kernel-Density-Estimator)

Flavour state assignment based on $M(K\pi)$ value

- mis-tagged event fraction 14%, measured on MC

Background component

- exponential mass shape
- polynomial shape for each angular variable
- factorisation of angular components tested

Fit algorithm

- Two-step fit performed for 7 (+2 control regions) q^2 bins:
  - fit m side bands to determine the background shape
  - fit whole mass spectrum with 5 floating parameters (2 yields, P_1, P_5', A_s^5)
- Unbinned extended maximum likelihood estimator used
  - find maximum of $\mathcal{L}$ inside the physically allowed region
- Statistical uncertainty using profiled Feldman-Cousins method
- Blind procedure: before fitting the signal mass region on data, the fit procedure has been fully tested and validated on simulation

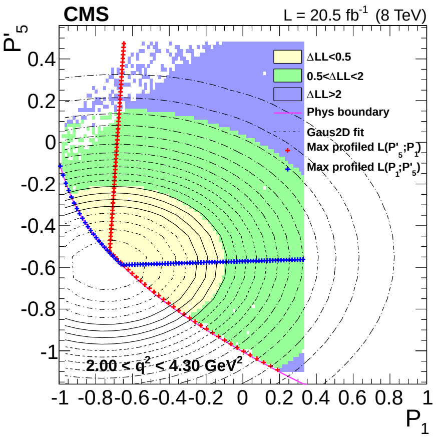

Systematic uncertainties

Source	$P_1 (\times 10^{-3})$	$P_5' (\times 10^{-3})$
Simulation mismodeling	1–33	10–23
Fit bias	5–78	10–120
Finite size of simulated samples	29–73	31–110
Efficiency	17–100	5–65
$K\pi$ mistagging	8–110	6–66
Background distribution	12–70	10–51
Mass distribution	12	19
Feed-through background	4–12	3–24
F_L, F_S, A_S uncertainty propagation	0–210	0–210
Angular resolution	2–68	0.1–12
Total	100–230	70–250

- **Fit bias** with cocktail signal MC + toy background from data side-bands
- **MC stat** due to limited statistics in efficiency shape evaluation
- **Efficiency**: comparing F_L on CR wrt PDG
- **$K\pi$ mistag** evaluated in J/ψ control region and propagated to all bins

Propagation of F_L, F_S, and A_s uncertainties:

- Generate pseudo experiments, with x100 events, for each q^2 bin
- Fit with F_L, F_S, A_s free to float and with F_L, F_S, A_s fixed
- Ratio of stat. uncert. on P_1 and P_5' with free and fixed fit used to estimate syst uncertainties

Results: fit projection for second bin: $2.0 < q^2 < 4.3\,\text{GeV}^2$

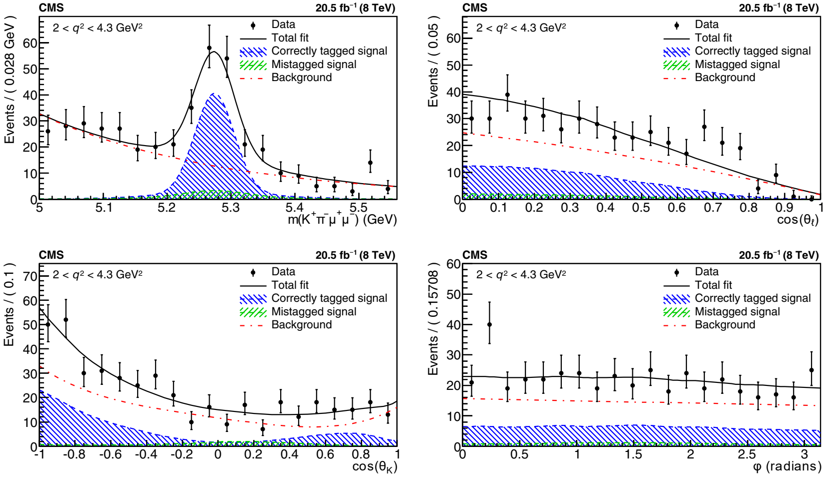

Results

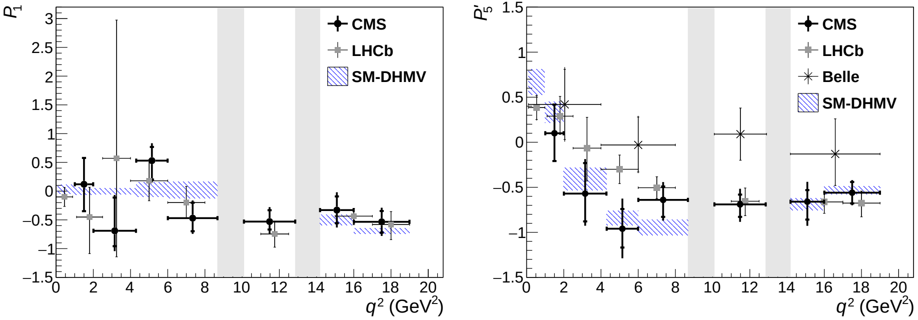

- SM-DHMV prediction computed using
  - soft form factors + parametrised power corrections
  - hadronic charm-loop contribution derived from calculations
- Results compatible with SM predictions within uncertainties
- No significant deviations from other experimental results

$B^+ \to K^+\mu^+\mu^-$ angular analysis

Phys. Rev. D 98 (2018) 112011
arXiv:1806.00636

- Fully described by the angle θ_ℓ and $q^2 = M^2_{\mu\mu}$;
- Angular decay rate:

$$\frac{1}{\mathrm{d}\Gamma/\mathrm{d}q^2}\frac{\mathrm{d}^2\Gamma}{\mathrm{d}q^2\mathrm{d}\cos\theta_l} = \frac{3}{4}(1-F_\mathrm{H})\left(1-\cos^2\theta_\ell\right)+\frac{1}{2}F_\mathrm{H}+\mathcal{A}_\mathrm{FB}\cos\theta_\ell$$

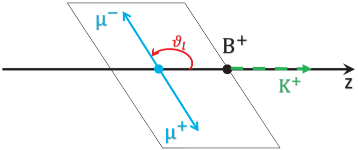

- Angular analysis to measure
  - angular parameter F_H
  - forward-backward asymmetry of the muons, $\mathcal{A}_{FB}$
- Range of q^2 divided in 9 bins
  - 7 signal bins
  - 2 bins for resonant decays $B^+ \to J/\psi K^+$ and $B^+ \to \psi(2S)K^+$ (control channels)
  - 2 additional special bins: [1-6] GeV^2 (clean predictions) and [1-22] GeV^2 (full signal)

Fit algorithm

$$\text{p.d.f.}(m, \cos\theta_l) = Y_S \cdot S_i(m) \cdot S_i^a(\cos\theta_l) \cdot \epsilon_i(\cos\theta_l) + Y_B \cdot B_i^m(m) \cdot B_i^{\cos\theta_l}(\cos\theta_l)$$

- Signal pdf component
  - double Gaussian mass shape
  - efficiency parameterised from MC with 6th-order polynomial
- Background pdf component
  - exponential mass shape
  - polynomial (3rd- or 4th-order) + Gaussian for the angular shape
- Two-step fit performed:
  - fit m side bands to determine the background shape (fixed in second step)
  - fit whole mass spectrum with 4 floating parameters (2 yields + 2 angular param)
- Unbinned extended maximum likelihood estimator used
- Statistical uncertainty using profiled Feldman-Cousins method

Validation and systematic uncertainties

Several validation steps

- With signal MC sample (both high statistics and data-like)
- With resonant control regions

Systematic uncertainty	A_{FB} ($\times 10^{-2}$)	F_H ($\times 10^{-2}$)
Finite size of MC samples	0.4–1.8	0.9–5.0
Efficiency description	0.1–1.5	0.1–7.8
Simulation mismodeling	0.1–2.8	0.1–1.4
Background parametrization model	0.1–1.0	0.1–5.1
Angular resolution	0.1–1.7	0.1–3.3
Dimuon mass resolution	0.1–1.0	0.1–1.5
Fitting procedure	0.1–3.2	0.4–25
Background distribution	0.1–7.2	0.1–29
Total systematic uncertainty	1.6–7.5	4.4–39

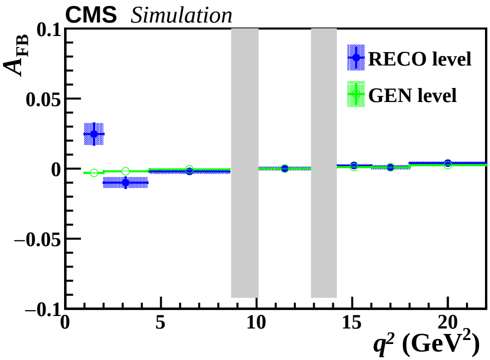

Dominant systematic uncertainty from background description

Results: fit projections for special bin $1 < q^2 < 6$ GeV^2

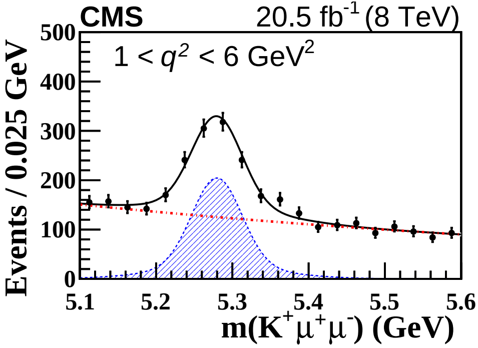

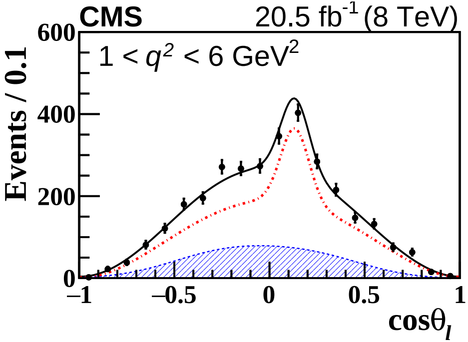

Results

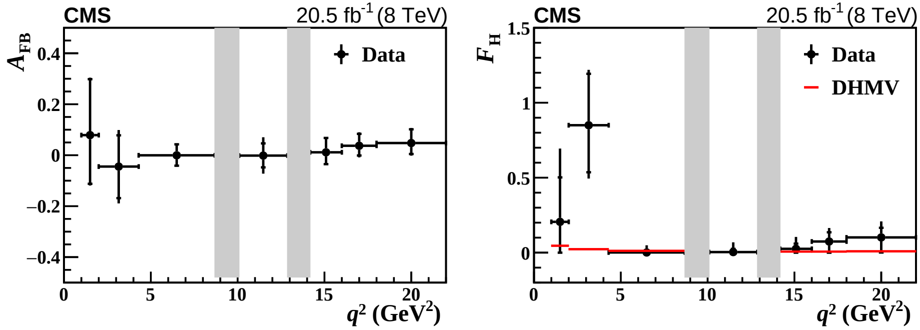

- Inner error bar is statistical uncertainty
- Full bar is total uncertainty
- Results compatible with SM predictions within uncertainties

Prospects for $B^0 \to K^{*0}\mu\mu$ analysis at HL-LHC

Report: CMS-PAS-FTR-18-033

- **Uncertainty on P_5'** measurement in $B^0 \to K^{*0}\mu\mu$ angular distribution is extrapolated to **HL-LHC** scenario at 3000 fb^{-1}
- Run 1 results used as baseline
- Upgraded CMS tracker detector provides improved mass resolution
- No changes in trigger performances and analysis strategy have been considered
- Signal yield has been obtained from MC simulations with Phase-2 detector upgrade and pileup of 200
  - Scaled to 3000 fb^{-1}: $\sim$ 700k events in the full q^2 range

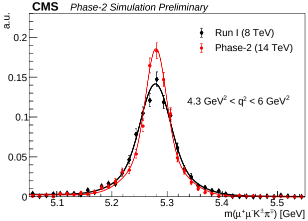

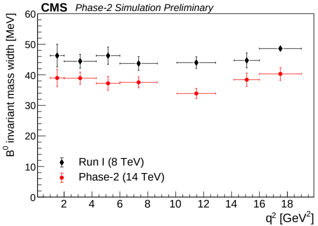

Projections on P'_5 uncertainty (HL-LHC)

- Run 1 statistical uncertainty scaled according to the expected yield
- Systematic uncertainties based on data control channel scaled according to statistics
- Other systematic uncertainties scaled by factor of 2
- Total uncertainty is expected to improve by 15 times wrt Run 1 result
- Large signal yield allows to split **q^2 range in finer bins**

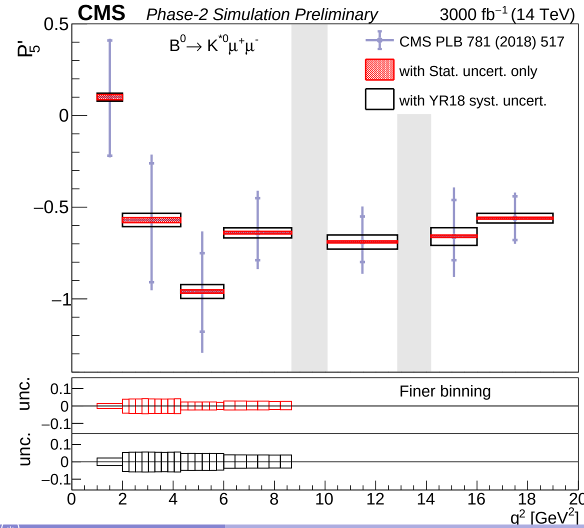

Summary

FCNC rare decays are being extensively studied in CMS

- $\mathrm{B}^0 \to \mathrm{K}^{*0}\mu\mu$ angular analysis has been extended to measure P_1 and P_5'
- $\mathrm{B}^+ \to \mathrm{K}^+\mu\mu$ angular analysis performed for the first time in CMS, to measure $\mathcal{A}_{\mathrm{FB}}$ and F_{H}
- Prospects of $\mathrm{B}^0 \to \mathrm{K}^{*0}\mu\mu$ angular analysis in HL-LHC

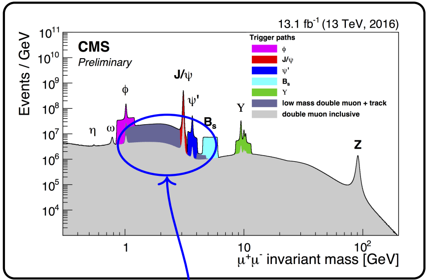

Currently working on Run 2 analyses

- dedicated trigger requiring two muons + 1 track with common vertex
- more decay channels to be explored
- Stay tuned

Backup slides

The validity range

To guarantee that the decay rate is always positively defined, the parameters have *physical boundaries*:

- interference terms $A_s^{(5)}$ have a definition range dependent on F_L, F_S, and P_1
- to have a positive P-wave component, P_1 and P_5' must satisfy: $(P_5')^2 - 1 < P_1 < 1$
  - purple line in the graph

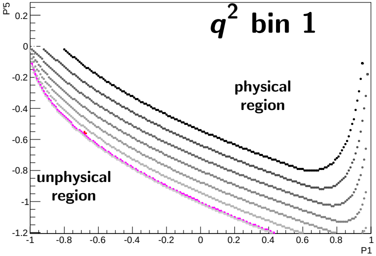

- to have a positive decay rate, an additional boundary need to be considered
  - depends on all the parameters
  - no analytic description available
  - computed numerically for each q^2 bin, using the fixed values of F_L, F_S, and A_s
  - grey lines in the graphs represent the boundary for different A_s^5 values within its range

Main cause of fit convergence problems → floating parameter A_s^5 and its influence on the physical boundary

Dataset selection for $B^0 \to K^{*0}\mu\mu$

Trig Dedicated HLT trigger path:
Low pt dimuon, displaced, low invariant mass

μ $p_T^{\mu} > 3.5$ GeV, $p_T^{\mu\mu} > 6.9$ GeV,
with high-quality displaced vertex

h $p_T^{h} > 0.8$ GeV, $|M(K\pi) - M_{K^{*0}}| < 90$ MeV,
$M_{KK} > 1.035$ (ϕ veto), displaced from the primary vertex

B^0 $p_t > 8$ GeV, $|\eta| < 2.2$, with four-body displaced vertex requirement and global momentum alignment

- both B^0 and $\overline{B}^0$ considered
- anti radiation cut against feed-down of $J/\psi/\psi(2S)$

CR : J/ψ and $\psi(2S)$ resonances used as control regions and treated in the same way.

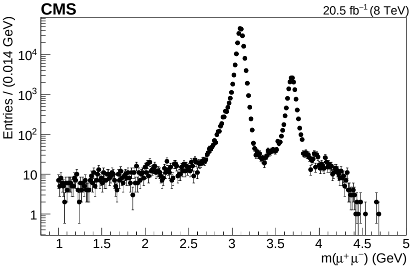

no PID to distinguish K from π,
flavour state assignment based on which hypothesis $M(K^+\pi^-/K^-\pi^+)$ is closer to $M_{K^{*0}}(PDG)$
mistag rate 14% (MC)

Anti-radiation cut

The signal sample is required to pass the selection:

- $m(\mu\mu) < m_{J/\psi PDG} - 3\sigma_{m(\mu\mu)}$ or
- $m_{J/\psi PDG} + 3\sigma_{m(\mu\mu)} < m(\mu\mu) < m_{\psi' PDG} - 3\sigma_{m(\mu\mu)}$ or
- $m(\mu\mu) > m_{\psi' PDG} + 3\sigma_{m(\mu\mu)}$;

for the control channel $B^0 \to K^{*0}(K^+\pi^-)J/\psi(\mu^+\mu^-)$ the requirement is:

- $|m(\mu\mu) - m_{J/\psi PDG}| < 3\sigma_{m(\mu\mu)}$.

while for the $B^0 \to K^{*0}(K^+\pi^-)\psi'(\mu^+\mu^-)$ channel is:

- $|m(\mu\mu) - m_{\psi' PDG}| < 3\sigma_{m(\mu\mu)}$.

To further reject feed-through from control channels ➜

Events are **rejected** if $m(\mu\mu) < m_{J/\psi PDG}$, then:

- $|(m(K\pi\mu\mu) - m_{B^0 PDG}) - (m(\mu\mu) - m_{J/\psi PDG})| < 160$ MeV/c^2;
- $|(m(K\pi\mu\mu) - m_{B^0 PDG}) - (m(\mu\mu) - m_{\psi' PDG})| < 60$ MeV/c^2;

while if $m_{J/\psi PDG} < m(\mu\mu) < m_{\psi' PDG}$, then:

- $|(m(K\pi\mu\mu) - m_{B^0 PDG}) - (m(\mu\mu) - m_{J/\psi PDG})| < 60$ MeV/c^2;
- $|(m(K\pi\mu\mu) - m_{B^0 PDG}) - (m(\mu\mu) - m_{\psi' PDG})| < 60$ MeV/c^2;

and if $m(\mu\mu) > m_{\psi' PDG}$, then:

- $|(m(K\pi\mu\mu) - m_{B^0 PDG}) - (m(\mu\mu) - m_{J/\psi PDG})| < 60$ MeV/c^2;
- $|(m(K\pi\mu\mu) - m_{B^0 PDG}) - (m(\mu\mu) - m_{\psi' PDG})| < 30$ MeV/c^2.

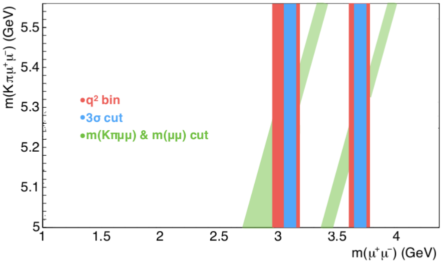

Efficiency and closure test (right tag)

- Numerator and denominator of efficiency are separately described with nonparametric technique implemented with a kernel density estimator on unbinned distributions
- Final efficiency distributions in the p.d.f. obtained from the ratio of 3D histograms derived from the sampling of the kernel density estimators

Closure test:

- compute efficiency with half of the MC simulation and use it to correct the other half
- same test performed both for correctly and mistagged events

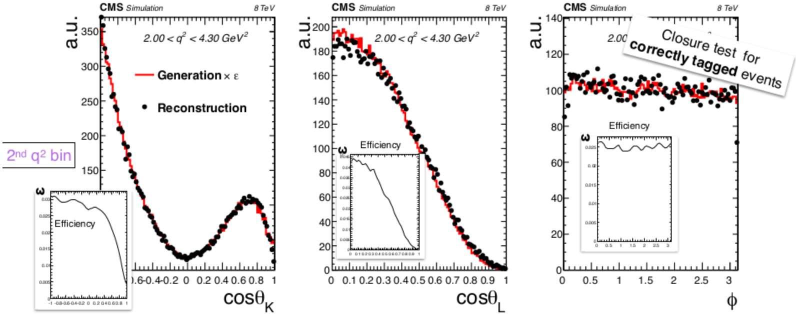

Efficiency and closure test (wrong tag)

- Numerator and denominator of efficiency are separately described with nonparametric technique implemented with a kernel density estimator on unbinned distributions
- Final efficiency distributions in the p.d.f. obtained from the ratio of 3D histograms derived from the sampling of the kernel density estimators

Closure test:

- compute efficiency with half of the MC simulation and use it to correct the other half
- same test performed both for correctly and mistagged events independently

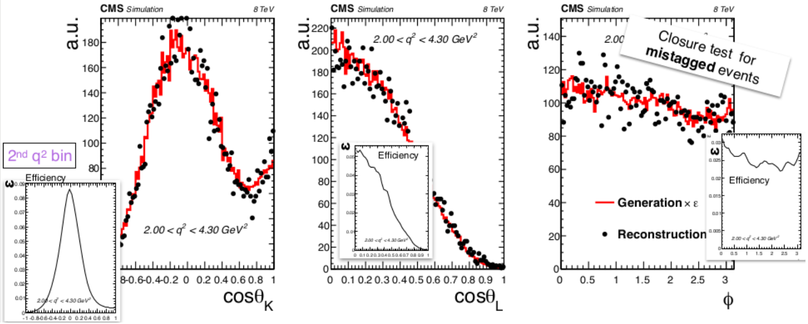

Background considered included:

- Partially reconstructed B^0 decay might pollute left M_{B^0} side bands
  - restrict left s.b. ($5.1 < M < 5.6$ GeV, default $5 < M < 5.6$ GeV)
  - redo fit: change in P_1 and P_5' within the systematic uncertainties.
- $B^\pm \to K^\pm\mu\mu$ plus and additional random $\pi^\mp$:
  - distribution ends at $M > 5.4$ GeV, further reduced by $\cos\alpha$ cut, and BR similar to $B^0 \to K^{*0}\mu\mu$
- $\Lambda_b \to pKJ/\psi(\mu^+\mu^-)$
  - look at event in the $M_{K\pi\mu\mu} \approx M_{B^0}$ peak, reconstruct them using p, K mass hypothesis: no peak seen.
- $B^0 \to DX$, with $D \to hh$ and h mis-id as μ
  - requires two mis-id: $P_{misId} \sim 1 \cdot 10^{-3}$: given $BR \sim 1 \cdot 10^{-3}$ negligible.
- $B^0 \to J/\psi(\mu\mu)K^{*0}(K\pi)$, with one h and one μ switched
  - $P_{misId\ \mu} \cdot (1 - \varepsilon_\mu) \sim 1 \cdot 10^{-4}$, $Y_{B^0 \to J/\psi\mu\mu} \sim 1.6 \cdot 10^5$: few events in bin close to J/ψ
  - J/ψ feed contamination in close bin included in the fit model

Fit validation

extensive fit validation with MC: used as **systematics**

- compare fit results with MC input values (**sim mismodeling**)
- compare with data-like MC (**fit bias**)
  - signal only correct tag
  - signal correct+wrong tag
  - signal + background
- Data control channel (J/ψ and $\psi(2S)$), comparing fit results with PDG (F_L) (**efficiency**)
- compare P_1 and P_5' on J/ψ and $\psi(2S)$ w/ and w/o F_L fixed: no bias

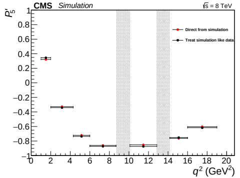

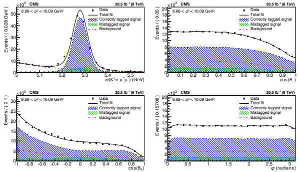

$$\frac{\mathcal{B}(B^0 \to K^{*0}\psi(2S))}{\mathcal{B}(B^0 \to K^{*0}J/\psi)} == \frac{Y_{\psi(2S)}}{\epsilon_{\psi(2S)}}\frac{\epsilon_{J/\psi}}{Y_{J/\psi}}\frac{\mathcal{B}(J/\psi \to \mu^+\mu^-)}{\mathcal{B}(\psi(2S) \to \mu^+\mu^-)} = 0.480 \pm 0.008(\mathrm{stat}) \pm 0.055(\mathrm{R}_\psi^{\mu\mu})$$

vs PDG $0.484 \pm 0.018(\mathrm{stat}) \pm 0.011(\mathrm{syst}) \pm 0.012(\mathrm{R}_\psi^{ee})$

Fit procedure

- The decay rate can become negative for certain values of the angular parameters (**P_1, P_5', A^5_s**)
- The presence of such a physically allowed region greatly complicates the numerical maximisation process of the likelihood by `MINUIT` and especially the error determination by `MINOS`, in particular next to the boundary between physical and unphysical regions
- The **best estimate** of **P_1** and **P_5'** is computed by:
  - discretise the bi-dimensional space **P_1-P_5'**
  - maximise the likelihood as a function of **Y_S**, **Y_B**, and **A^5_s** at fixed values of **P_1**, **P_5'**
  - fit the likelihood distribution with a 2D-gaussian function
  - the maximum of this function inside the physically allowed region is the best estimate
- To ensure correct coverage for the **uncertainties** of **P_1** and **P_5'**, the Feldman-Cousins method is used in a simplified form: the confidence interval's construction is performed only along two 1D paths determined by profiling the 2D-gaussian description of the likelihood inside the physically allowed region

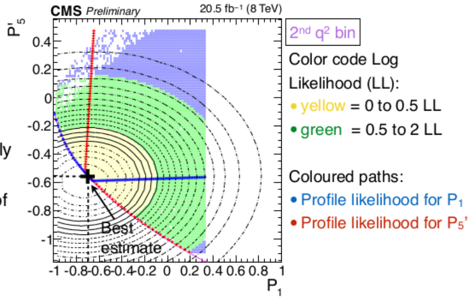

FC stat uncertainties determination

- To ensure correct coverage for the **uncertainties** of P_1 and P_5', the Feldman-Cousins method is used in a simplified form: the confidence interval's construction is performed only along the two 1D paths determined by profiling the 2D-gaussian description of likelihood inside the physically allowed region:
  - generate 100 pseudo-experiments for each point of the path
  - fit and rank according to the likelihood-ratio
  - confidence interval bound is found when data likelihood-ratio exceeds the 68.3% of the pseudo-experiments

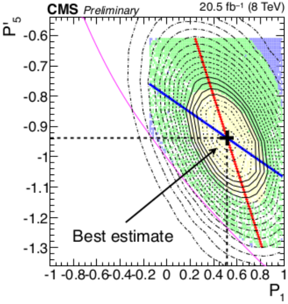

- Due to the limited number of pseudo-experiments statistical fluctuations are present
- To produce a robust result, the ranking of the data likelihood-ratio is plotted for several scan points
- The intersection is then computed using a linear fit

CMS results (table)

q^2 (GeV^2)	Signal yield	P_1	P'_5	Correlations
1.00–2.00	80 ± 12	$+0.12\ ^{+0.46}_{-0.47} \pm 0.10$	$+0.10\ ^{+0.32}_{-0.31} \pm 0.07$	-0.0526
2.00–4.30	145 ± 16	$-0.69\ ^{+0.58}_{-0.27} \pm 0.23$	$-0.57\ ^{+0.34}_{-0.31} \pm 0.18$	-0.0452
4.30–6.00	119 ± 14	$+0.53\ ^{+0.24}_{-0.33} \pm 0.19$	$-0.96\ ^{+0.22}_{-0.21} \pm 0.25$	$+0.4715$
6.00–8.68	247 ± 21	$-0.47\ ^{+0.27}_{-0.23} \pm 0.15$	$-0.64\ ^{+0.15}_{-0.19} \pm 0.13$	$+0.0761$
10.09–12.86	354 ± 23	$-0.53\ ^{+0.20}_{-0.14} \pm 0.15$	$-0.69\ ^{+0.11}_{-0.14} \pm 0.13$	$+0.6077$
14.18–16.00	213 ± 17	$-0.33\ ^{+0.24}_{-0.23} \pm 0.20$	$-0.66\ ^{+0.13}_{-0.20} \pm 0.18$	$+0.4188$
16.00–19.00	239 ± 19	$-0.53 \pm 0.19 \pm 0.16$	$-0.56 \pm 0.12 \pm 0.07$	$+0.4621$

Fit Projections

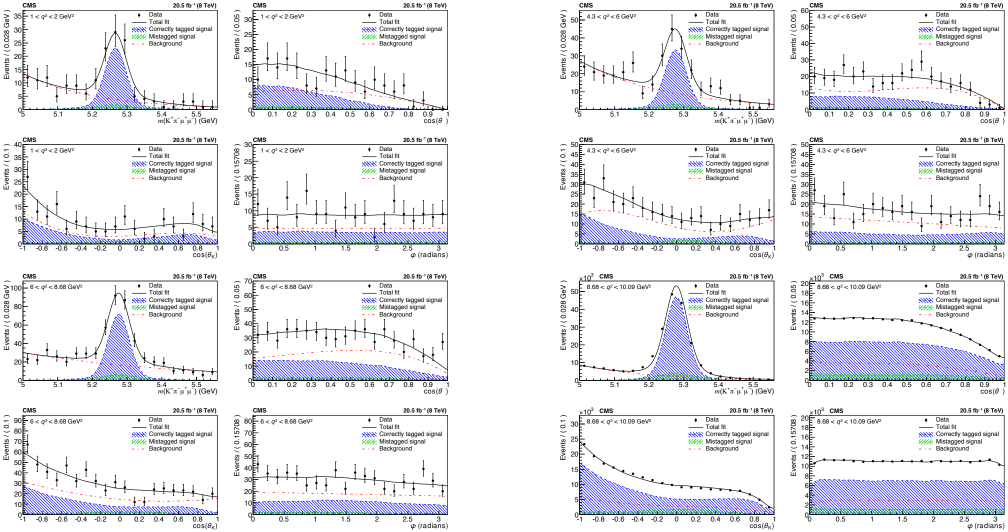

Fit Projections

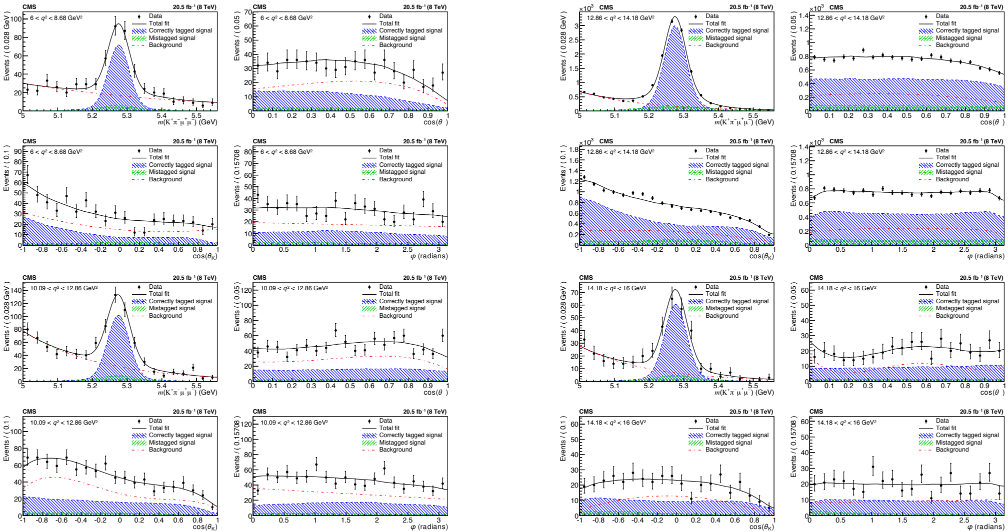

Decay rate

$$\frac{d^4\Gamma[\bar{B}^0 \to \bar{K}^{*0}\mu^+\mu^-]}{dq^2\, d\vec{\Omega}} = \frac{9}{32\pi} \sum_i I_i(q^2) f_i(\vec{\Omega})$$ → Decay rate involving b quark, *i.e.* B^0_{bar} meson

$$\frac{d^4\bar{\Gamma}[B^0 \to K^{*0}\mu^+\mu^-]}{dq^2\, d\vec{\Omega}} = \frac{9}{32\pi} \sum_i \bar{I}_i(q^2) f_i(\vec{\Omega})$$ → Decay rate involving b_{bar} quark, *i.e.* B^0 meson

- Γ and Γ_{bar}: expression of the decay
- $f(\vec{\Omega})$: combinations of spherical harmonics
- I and I_{bar}: q^2-dependent angular parameters (combinations of six complex decay amplitudes)

$$\frac{1}{d(\Gamma+\bar{\Gamma})/dq^2} \frac{d^4(\Gamma+\bar{\Gamma})}{dq^2\, d\vec{\Omega}} = \frac{9}{32\pi}\Big[\frac{3}{4}(1-F_L)\sin^2\theta_K + F_L\cos^2\theta_K + \frac{1}{4}(1-F_L)\sin^2\theta_K\cos 2\theta_l - F_L\cos^2\theta_K\cos 2\theta_l + S_3\sin^2\theta_K\sin^2\theta_l\cos 2\phi + S_4\sin 2\theta_K\sin 2\theta_l\cos\phi + S_5\sin 2\theta_K\sin\theta_l\cos\phi + \frac{4}{3}A_{FB}\sin^2\theta_K\cos\theta_l + S_7\sin 2\theta_K\sin\theta_l\sin\phi + S_8\sin 2\theta_K\sin 2\theta_l\sin\phi + S_9\sin^2\theta_K\sin^2\theta_l\sin 2\phi\Big]$$

Assumptions / simplifications:

- CP-averaged measurement
- Massless limit, *i.e.* $q^2 \gg 4m^2_\mu$

↓

8 independent angular parameters

Decay rate

Decay rate parameterisation
(*JHEP 01 (2013) 048*)

For example $P_5' = \frac{S_5}{\sqrt{F_L(1-F_L)}}$

$$\frac{d^4\Gamma}{dq^2\, d\cos\theta_K\, d\cos\theta_l\, d\phi} = \frac{9}{32\pi}\Big[\frac{3}{4}F_L \sin^2\theta_K + F_L\cos^2\theta_K + (\frac{1}{4}F_L\sin^2\theta_K - F_L\cos^2\theta_K)\cos 2\theta_l + \frac{1}{2}P_1 F_L \sin^2\theta_K\sin^2\theta_l\cos 2\phi + \sqrt{F_L F_L}\left(\frac{1}{2}P_4'\sin 2\theta_K \sin 2\theta_l\cos\phi + P_5'\sin 2\theta_K\sin\theta_l\cos\phi\right) - \sqrt{F_L F_L}\left(P_6'\sin 2\theta_K\sin\theta_l\sin\phi - \frac{1}{2}P_8'\sin 2\theta_K\sin 2\theta_l\sin\phi\right) + 2P_2F_L\sin^2\theta_K\cos\theta_l - P_3F_L\sin^2\theta_K\sin^2\theta_l\sin 2\phi\Big] = \frac{d\Gamma^4_{\text{P-wave}}}{dq^2\, d\Omega}$$

Two channels can contribute to the final state $K^+ \pi^- \mu^+ \mu^-$:

- P-wave channel, $K^+ \pi^-$ from the meson vector resonance K^{*0} decay
- S-wave channel, $K^+ \pi^-$ not coming from any resonance

We have to parametrise both decay rates !

$$\frac{d\Gamma^4_{\text{Total}}}{dq^2\, d\Omega} = (1 - F_S)\frac{d\Gamma^4_{\text{P-wave}}}{dq^2\, d\Omega} + \frac{d\Gamma^4_{\text{S/SP-wave}}}{dq^2\, d\Omega}$$

Both S-wave and S&P wave interference

6 independent parameters

$$\frac{d\Gamma^4_{\text{S/SP-wave}}}{dq^2\, d\Omega} = \frac{3}{16\pi}\Big[F_S\sin^2\theta_\ell + A_S\sin^2\theta_\ell\cos\theta_K + A_S^4\sin\theta_K\sin 2\theta_\ell\cos\phi + A_S^5\sin\theta_K\sin\theta_\ell\cos\phi + A_S^7\sin\theta_K\sin\theta_\ell\sin\phi + A_S^8\sin\theta_K\sin 2\theta_\ell\sin\phi\Big]$$

Efficiency parameterisation - $B^+ \to K^+\mu\mu$

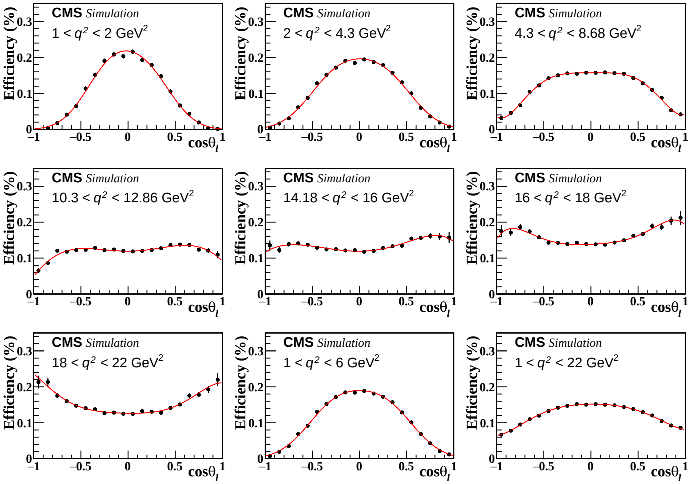

Fit projections - B^+-candidate mass

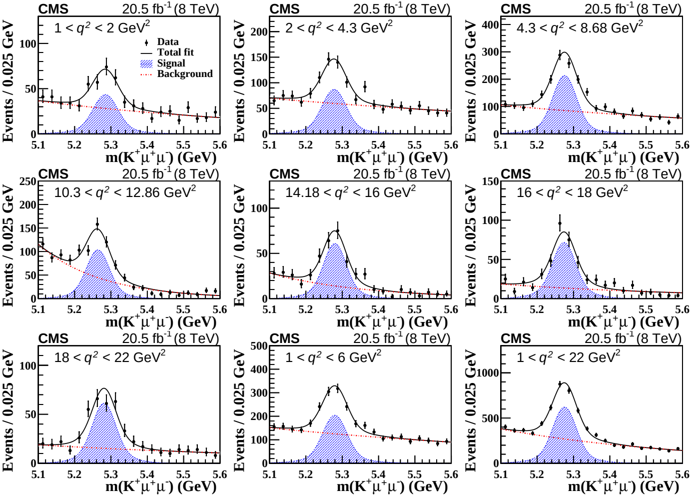

Fit projections - $\cos\theta_\ell$

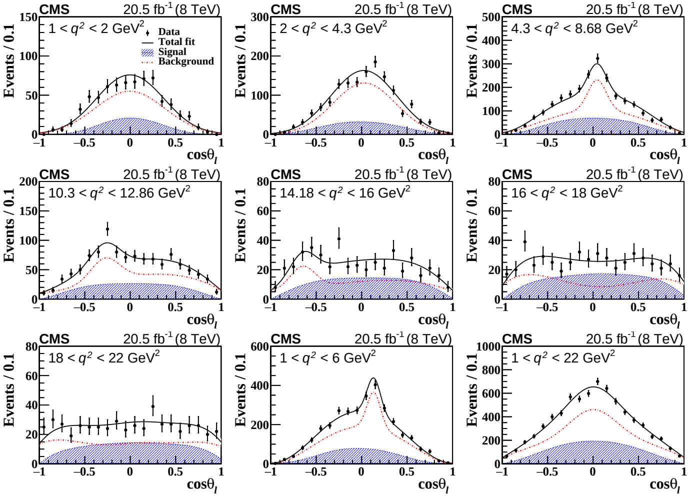

Fit results - $B^+ \to K^+ \mu\mu$

q^2 (GeV^2)	Y_S	A_{FB}	F_H	F_H(EOS)	F_H(DHMV)	F_H(FLAVIO)
1.00–2.00	169 ± 22	$0.08\,^{+0.22}_{-0.19} \pm 0.05$	$0.21\,^{+0.29}_{-0.21} \pm 0.39$	0.047	0.046	0.045
2.00–4.30	331 ± 32	$-0.04\,^{+0.12}_{-0.12} \pm 0.07$	$0.85\,^{+0.34}_{-0.31} \pm 0.14$	0.024	0.023	0.022
4.30–8.68	785 ± 42	$0.00\,^{+0.04}_{-0.04} \pm 0.02$	$0.01\,^{+0.02}_{-0.01} \pm 0.04$	—	0.012	0.011
10.09–12.86	365 ± 29	$0.00\,^{+0.05}_{-0.05} \pm 0.05$	$0.01\,^{+0.02}_{-0.01} \pm 0.06$	—	—	—
14.18–16.00	215 ± 19	$0.01\,^{+0.06}_{-0.05} \pm 0.02$	$0.03\,^{+0.03}_{-0.03} \pm 0.07$	0.007	0.007	0.006
16.00–18.00	262 ± 21	$0.04\,^{+0.05}_{-0.04} \pm 0.03$	$0.07\,^{+0.06}_{-0.07} \pm 0.07$	0.007	0.007	0.006
18.00–22.00	226 ± 20	$0.05\,^{+0.05}_{-0.04} \pm 0.02$	$0.10\,^{+0.06}_{-0.10} \pm 0.09$	0.008	0.009	0.008
1.00–6.00	778 ± 47	$-0.14\,^{+0.07}_{-0.06} \pm 0.03$	$0.38\,^{+0.17}_{-0.21} \pm 0.09$	0.025	0.025	0.020
1.00–22.00	2286 ± 73	$0.00\,^{+0.02}_{-0.02} \pm 0.03$	$0.01\,^{+0.01}_{-0.01} \pm 0.06$	—	—	—

Experiment comparison